Strain-dependent stretch-activated ion channel in Hodgkin-Huxley-form models of ventricular cardiomyocyte action potential

Christopher Villongco

Emily Pfeiffer

December 10, 2010

BENG 260: Neurodynamics

Final Project Paper

Abstract

The electrophysiology of cardiac myocytes is tightly coupled to mechanics. One aspect of this is apparent in the effects of mechanical strain on cardiac action potential dynamics. These can be considered through adjustments to classic electrophysiological models. The standard FitzHugh Nagumo model is a reduced two-variable model from Hodgkin-Huxley that can reproduce basic mechanisms of action potential dynamics. A modified formulation that adapts the model to ventricular cardiomyocytes is considered. The Luo-Rudy model is also a Hodgkin-Huxley-derived model for action potentials driven by ionic currents in cardiac myocytes.

The Healy-McCulloch model predicts a decrease in time for 20% action potential repolarization and variable time for 90% action potential duration as seen in rabbit ardiomyocytes based on tiered conductance values. Recently, Lunze and Leonhardt provide a mathematical relation for stretch-activated conductance and strain in smooth muscle. This paper determines whether the Lunze-Leonhardt model for stretch-activation of ionic currents can be applied to a cardiomyocyte model. Using Matlab and Continuity, we will develop a modified model derived from the FitzHugh Nagumo and Luo-rudy models by incorporating a strain-dependent ion channel. We will simulate several coupled cardiomyocytes in Matlab with this modified model to reproduce the results of the Healy-McCulloch model. The modified FitzHugh Nagumo model is also implemented in a finite element simulation study the effects of a strain field on action potential propagation.

Introduction

The heart is essentially a mechanically functioning organ which primarily pumps blood though the body's circulation. Coordination of the timing and forces of contraction are vital to maintaining healthy cardiac pump function. As in skeletal muscle action potentials cause cardiac muscle to contract by releasing calcium ions into the myoplasm via voltage-gated calcium channels. These action potentials propagate along the conduction pathway of the heart in order to properly coordinate of the heart as a whole. Action potentials originate from the sinus node on the right atrium and traverse the atria to the atrioventricular (AV) node. This causes the myoctes in the atria to contract first by pumping their blood volume into the ventricles. The action potentials then travel down the bundle branches of the septum and enter the fast Purkinje fiber system in the ventricles, causing the ventricular myocytes to contract and pump blood through the pulmonic and systemic circulation circuits.

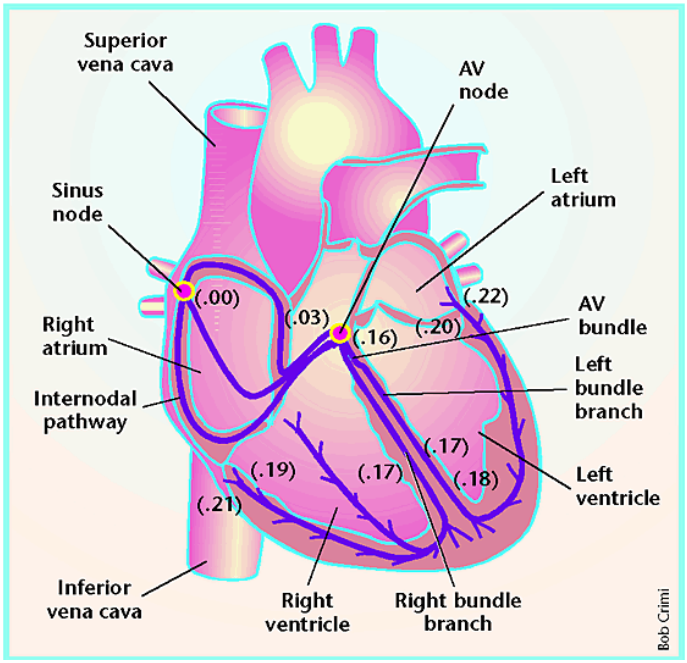

Figure 1: Schematic of the electrical conduction system of the heart.

The electrophysiological properties of cardiac myoctes are tightly coupled to mechanics. One aspect of this is apparent in the effects of myocyte mechanical strain on cardiac action potential dynamics. This phenomenon is known as mechanoelectric feedback (MEF). The mechanisms underlying MEF include mechanical modulation of intracellular calcium handling and stretch activation of ion channels. Physiologically, the influence of stretch activated currents (SACs) have been implicated in arrhythmias due to abnormal electric activity associated with increased pressure or volumic hemodynamic loading of the ventricles as observed in diseases such as hypertension, aortic valve disease, and congestive heart failure (Healy 2005).

Recently, Lunze and Leonhardt formulated a Hodgkin-Huxley type mathematical relation for stretch-activated current I'_M in smooth muscle (Lunze 2009):

$$I'_M = G_{stretch} \cdot P_m \cdot (V_m - E_{stretch}) \cdot A'_F$$

where $G_{stretch}$ is the channel conductance, P_m is the probability of the channel in the open state, V_m is the membrane potential, $E_{stretch}$ is the reversal potential of the channel, and A_F is an amplification factor which takes into account the density of the myocytes in a section of tissue. The open channel probability is formulated as:

$$P_m = \frac{1.0}{1 + e^{-\left(\frac{\varepsilon - \varepsilon_{1/2}}{k'_\varepsilon}\right)}}$$

where ε is strain, $\varepsilon'_{1/2}$ is the strain at which the open channel probability is 50%, and k'_ε determines the slope of the curve. Because a physiological amount of strain in a normal beating heart is typically about 20% during diastole, $\varepsilon'_{1/2}$ was set to 0.233 as was originally by Lunze and Leonhardt. The value for k'_ε was 0.018 as reported by Lunze.

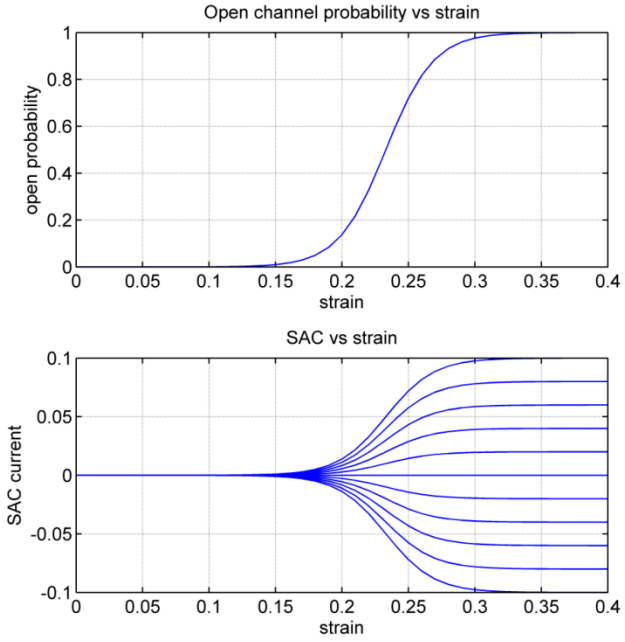

Figure 2: Top: The open-channel probability curve P_m. Bottom: The change in SAC current I'_M with increasing channel reversal potential $E_{stretch}$ (bottom curve to top curve).

The work presented in this paper considers the effects of incorporating the Lunze-Leonhardt SAC model in several standard models of cardiac action potentials. The FitzHugh-Nagumo model is a very simple two-variable model and is modified specifically for ventricular cardiomyocytes in this paper (Rogers 1995, FitzHugh 1961). More complex and

updated models incorporating recent ion channel data such as the Luo-Rudy model (Luo 1991) with eight transmembrane currents and the Healy-McCulloch model for stretch-activated currents in rabbit cardiomyocytes (Healy 2005) are more appropriate models in which to observe the effect of a SAC model.

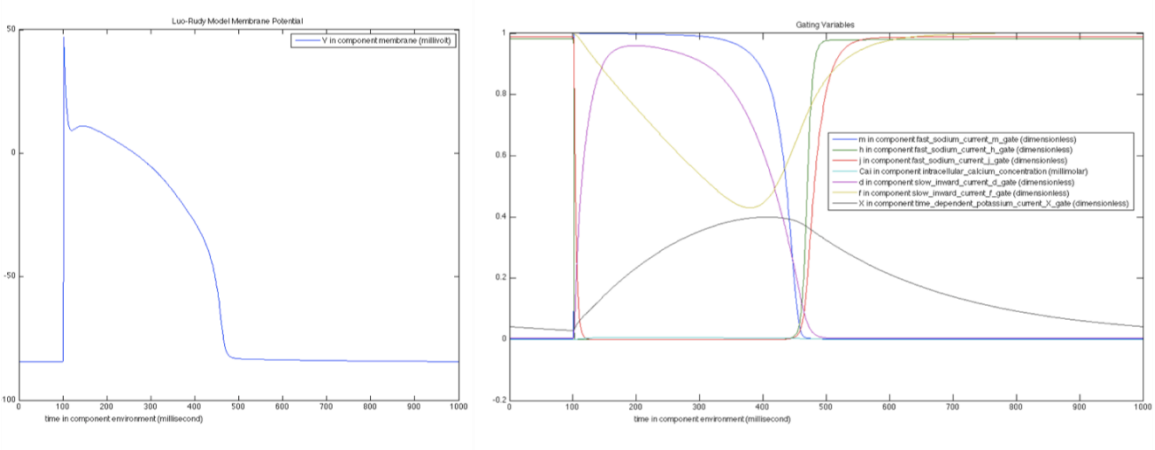

Figure 3: Luo-Rudy model membrane potential and gating variables. Currents include: I_{St} stimulus current, I_{Na} fast sodium current (m,h,j), I_{Si} slow inward current (d,f, Ca_i), I_K time-dependent potassium current (X), I_{K1} time-independent, concentration-dependent potassium current, I_{Kp} plateau potassium current, I_b time-independent background leakage current.

An extension of the twenty-variable Puglisi-Bers model, the Healy-McCulloch model predicts a decrease in time for the 20% action potential repolarization and variable time for 90% action potential duration as seen in rabbit cardiomyocytes based on tiered conductance values (Puglisi 2001, healy 2005). This paper determines whether the Lunze-Leonhardt model for stretch-activation of ionic currents can be applied to a cardiomyocyte model.

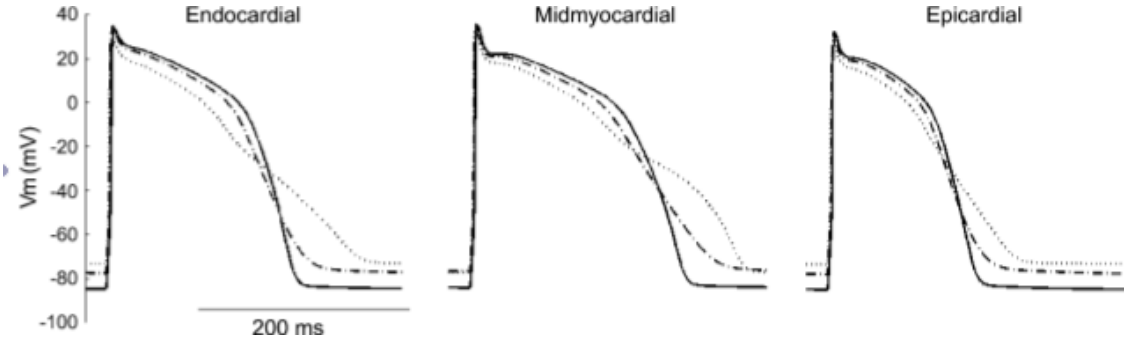

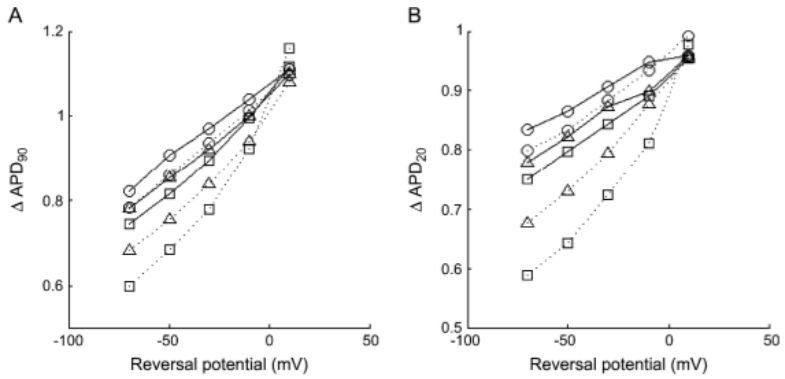

Figure 4: The Healy-McCulloch model shows APD20 shortening with the addition of a stretch-activated ion channel, with increasing effect as the channel reversal potential is lowered. In contrast, APD90 in this model shortens for lower channel reversal potentials but lengthens for reversal potentials higher than ~ 0 mV. In both cases, variability is seen among epicardial and endocardial cells (Adapted from Healy 2005).

Aims/Method

Using Matlab and Continuity, we will develop models of cardiac action potentials derived from the modified FitzHugh Nagumo and Luo-Rudy standard models by incorporating the Lunze-Leonhardt SAC model. We will simulate a single action potential event produced by an initial external stimulus for a single cardiomyocyte in Matlab to determine the effect of different magnitudes of a prescribed, time-independent strain as well as different reversal potentials for the SAC channel. The simulations will show whether or not the models can reproduce the same effects predicted by the Healy-McCulloch. Parameter values for channel conductance and amplification factor in the SAC varied and were estimated based on producing a SAC on the same order of magnitude as the dominant currents in the model.

We will also apply the modified FitzHugh Nagumo model to a finite element simulation of action potential propagation over excitable isotropic media in Continuity to observe the effects of homogenous strain on conduction. A 22x22 finite element mesh will be stimulated by an external current in its center for two cases: one without strain and one with a homogenous strain applied to the bottom half of the mesh. Whereas the Matlab simulations only consider the temporal effects of SACS on action potentials, the finite element simulation also takes into account the spatial effects.

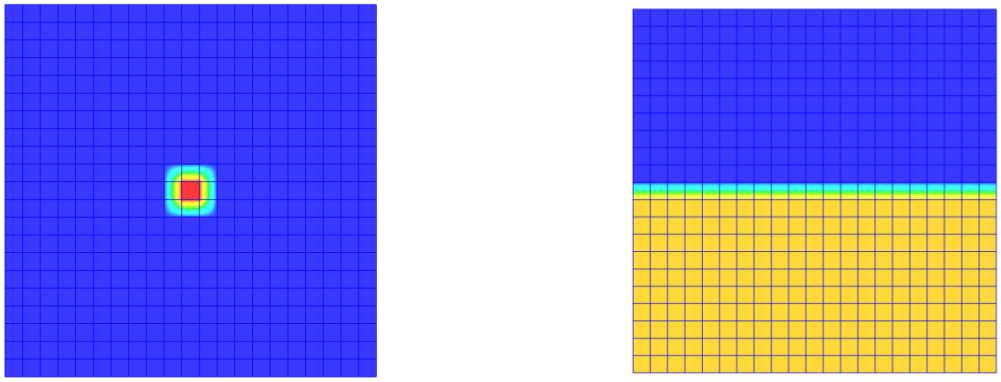

Figure 5: A 22x22 mesh is stimulated at its four nodes in the center of the square (left). Propagation will be compared between a mesh without strain and a mesh with a homogenous strain field (18%) (right) in the lower half of the square.

Results

Modified Fitzhugh Nagumo

Strain was varied in the operating range of open-channel probability curve (0.16 – 0.32). Since the MFHN quantifies a normalized excitable variable, the parameters chosen for the model were arbitrary and were selected by ensuring that the qualitative behavior was reasonably physiological. The simulation was allowed to run for 1 second with a 10 ms external stimulus applied at 200 ms. The SAC stimulus and excitable and recovery variables all exhibit the same trend in increasing strain: the magnitude of the change is small at the upper and lower bounds of the strain range and large in middle of the range. This variation is indicative of the influence of the behavior of the open-channel probability curve.

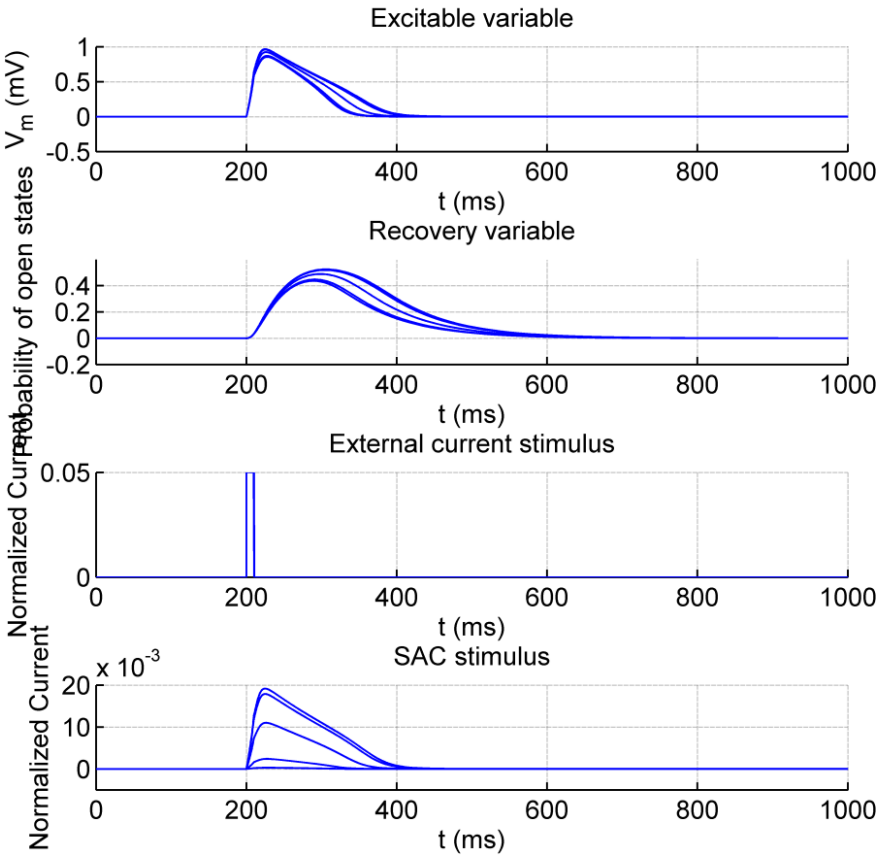

Figure 6: Effect of increasing magnitude strain magnitude from (0.16 to 0.32 in steps of 0.04) on excitation and recovery dynamics. The dependence of the SAC stimulus on the excitable variable is made clear by the similarly shaped time courses of the two curves.

The variation of APD20 (30 ms – 35.5 ms) and APD90 (101.75 ms – 156.25 ms) between strain magnitudes of 0.16 and 0.32 is shown in Figure 6. The two curves also share the same general trend in APD. The greatest change occurs in the intermediate strain range. This is again evidence of the influence of the general shape of the open-channel probability curve. There is no change in resting potential with change in strain.

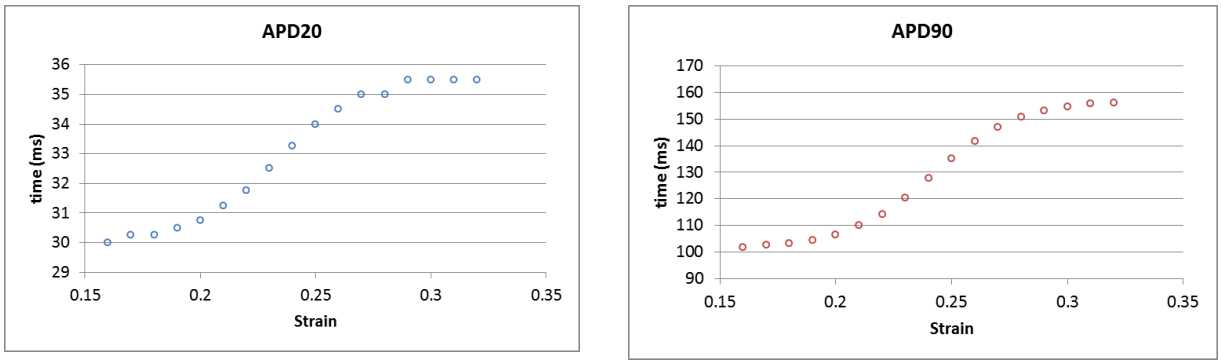

Figure 7: Change in APD 20 and APD 90 over strain ranges in steps of 0.01. The profiles of the two curves similarly resemble that of the open-channel probability curve. Note, however, the much larger variation of APD90 over the same strain range.

The effect of changes in reversal potential (0 – 1) of the stretch-activated channel was observed for strain magnitudes of 0.16 and 0.23. There was virtually no change in APD or resting potential for the case of 0.16 strain. Though the SAC was primarily affected, it changed in insignificant amounts, thus producing no significant differences due to reversal potential.

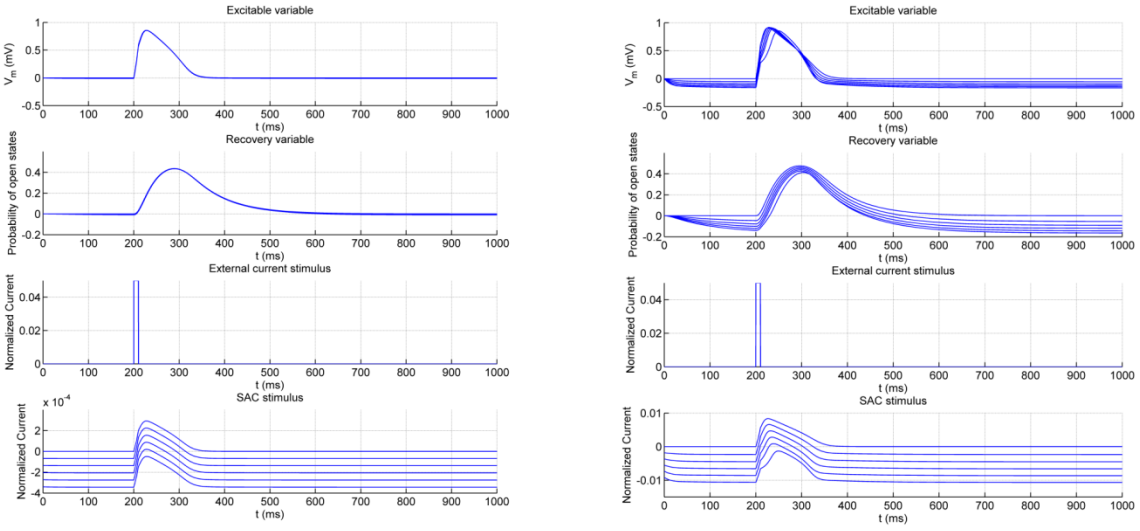

Figure 8: Effect of channel reversal potential ranging from 0 to 1 in steps of 0.2 on excitation and recovery dynamics and resting potential for 16% strain (left) and 23% strain (right).

However, at a strain magnitude of 0.23 the effects are much more pronounced. Figure 9 shows more clearly a linear decrease of resting potential (0 to -0.17), ADP20 (32.5 to 27.75),

and APD90 (120.5 to 76) with increased reversal potential. This linearity is due to the ohmic Hodgkin-Huxley-type formulation of the SAC with respect to reversal potential.

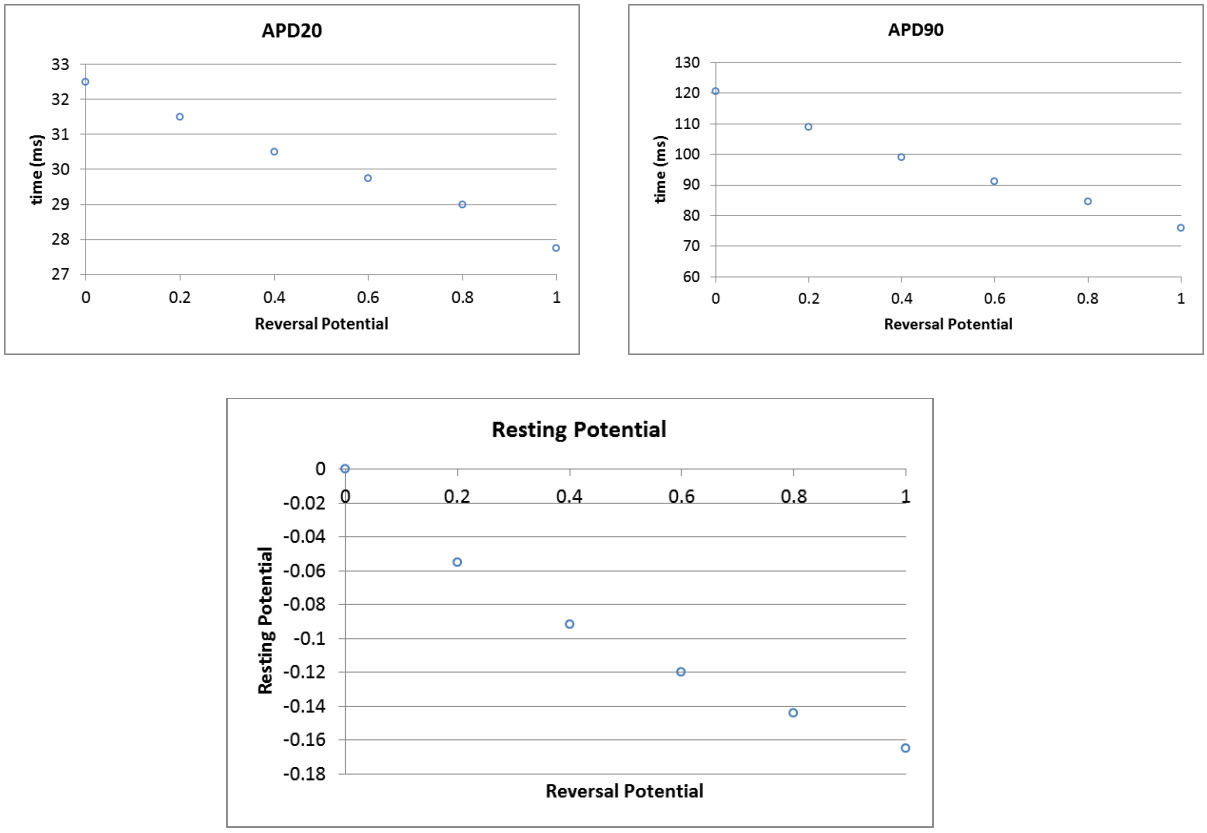

Figure 9: Variation of APD20, APD90, and resting potential with reversal potential at a strain magnitude of 0.23.

The results of the finite element simulation of action potential propagation on isotropic excitable media are shown in Figure 10. The simulation was run for 300 ms with external stimulus applied at time t=0 ms for 3 ms. In the baseline case (zero strain), the action potential conducts uniformly and monotonically across the square. When a constant strain of 18% is applied to the lower half of the square, the wave propagates with greater amplitude and velocity through the strained area. The wave in the upper part of square conducts as it normally did in the baseline isotropic case.

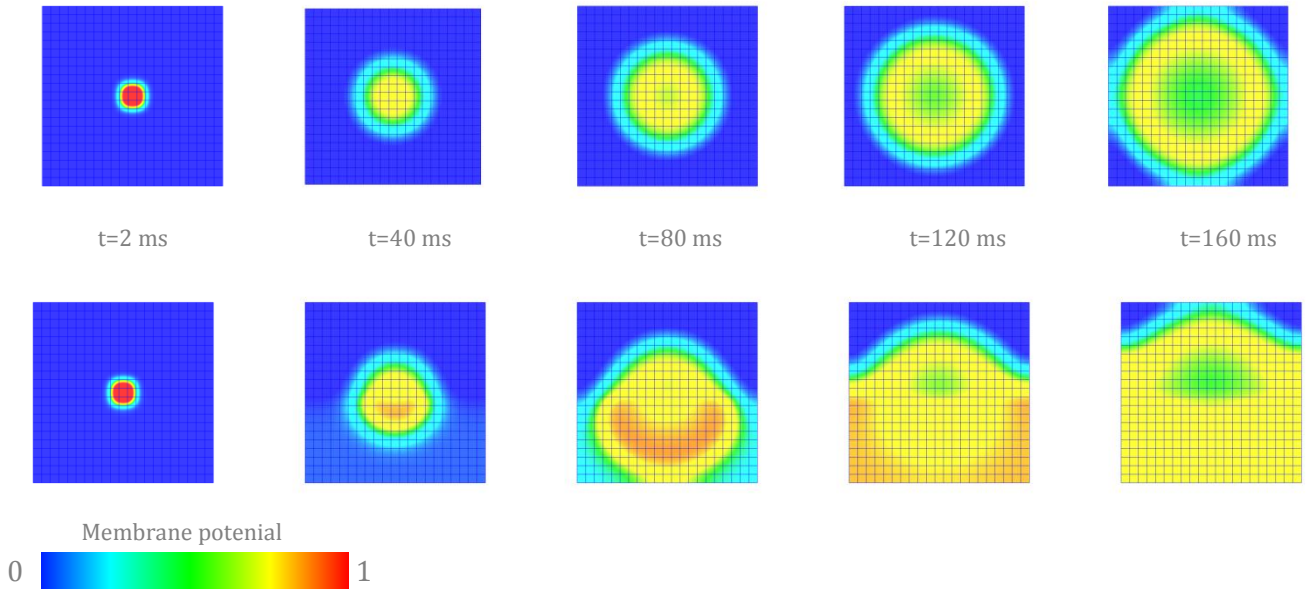

Figure 10: Finite element simulations of the excitatory variable by the modified FitzHugh Nagumo model across isotropic media without strain (top) and with 18% strain (bottom) applied to the lower half of the square. Only the first 160 ms is shown to illustrate the behavior of the wavefront before the entire square has been activated.

Modified Luo-Rudy

The addition of a strain-dependent, stretch-activated channel to the Luo-Rudy model markedly altered duration and shape of membrane depolarization. At sufficiently high strain states to facilitate channel opening, the stretch activated current is of comparable magnitude to those carried by other ionic channels in the Luo-Rudy model.

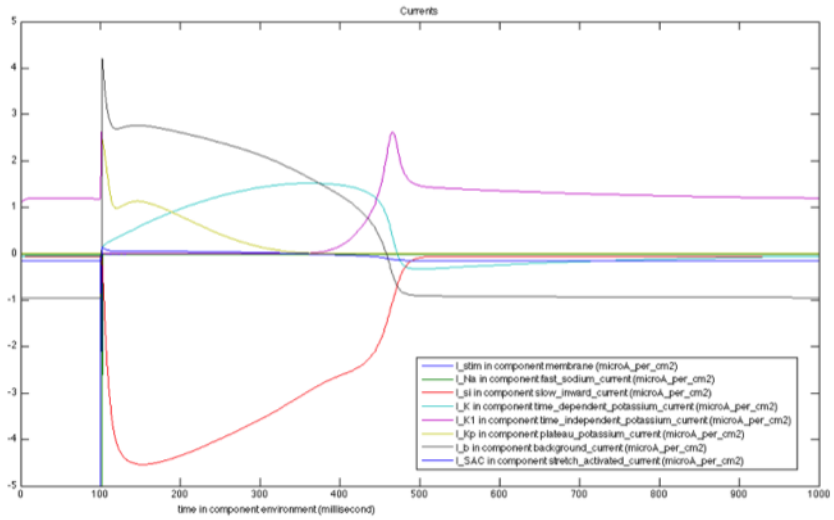

Figure 11: At 15% strain, the modified Luo-Rudy model shows a positive stretch-activated current through small channel opening at the initial depolarization with fast decay, followed by a small negative current at the time of membrane potential repolarization.

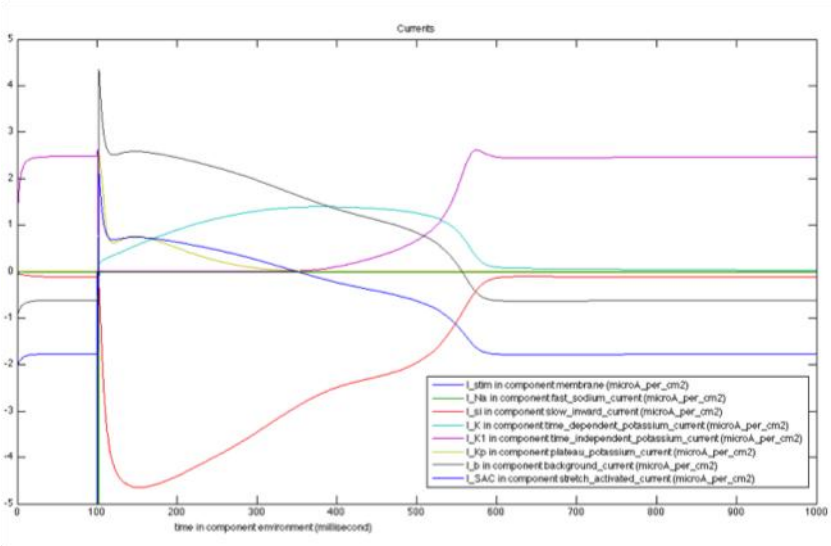

Figure 12: At 20% applied strain, the stretch-activated channel opens more significantly, allowing a potential-driven current comparable in magnitude to other cation currents described by the Luo-Rudy model. This current is positive during membrane depolarization and negative during later phases of repolarization.

At a stretch-activated channel reversal potential of -18 mV, the shortening in APD20 and lengthening of APD90 predicted by the Healy-McCulloch model for high reversal potentials is observed.

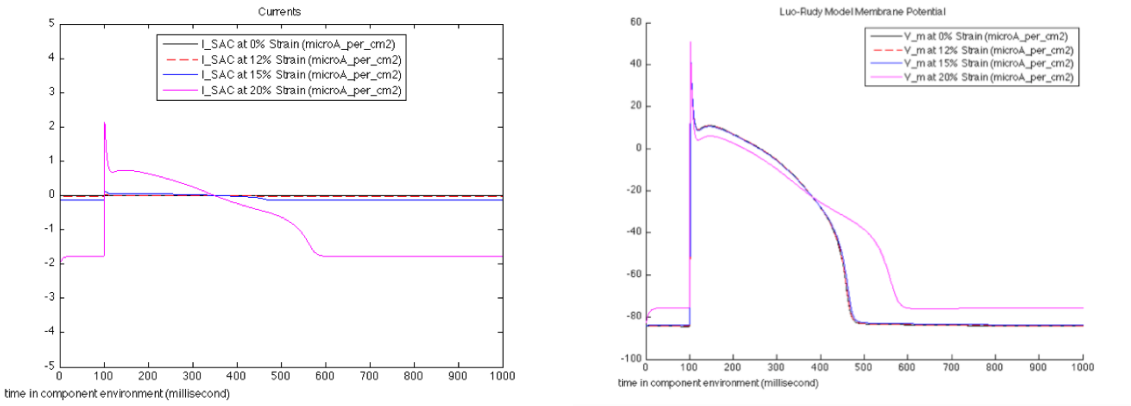

Figure 13 : The channel-opening effect of strain on the stretch-activated channel current and subsequent changes in membrane potential are only slightly detected at 15% strain, but important at 20% strain. APD20 shortening and APD90 lengthening as a result of the stretch-activated current (reversal potential -18 mV) are observed.

When stretch-activated current reversal potential is decreased to -60 mV, shortening of both APD20 and APD90 are observed.

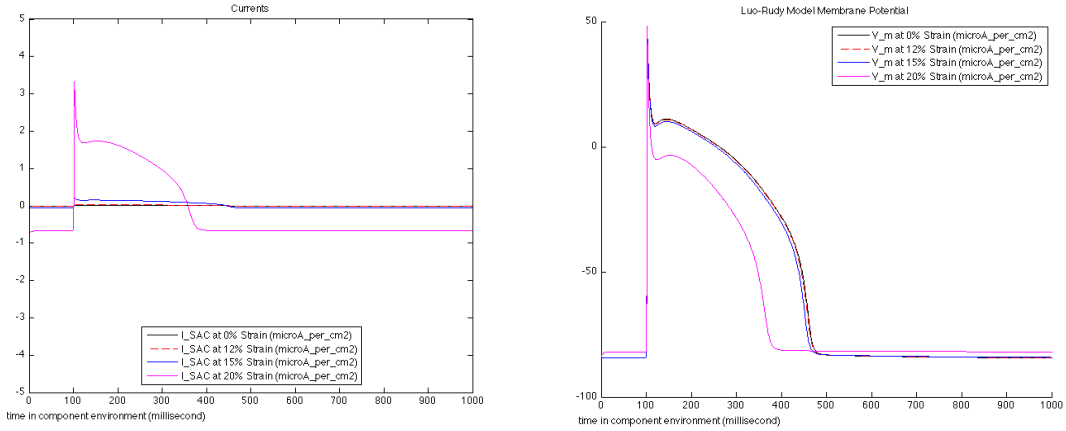

Figure 14: Luo-Rudy model with stretch-activated channel added, reversal potential -60 mV. Channel current and membrane potential examined at applied strains of 0, 10, 12, 15 and 20%.

Discussion

The original Fitzhugh Nagumo model for neuronal action potentials consists of only two state variables: one for excitation (u) representing transmembrane potential and one for recovery (v). Unlike neurons, cardiac myocytes do not hyperpolarize during the refractory period of an action potential. The modified Fitzhugh Nagumo (MFHN) takes this important feature into account by a modification of the excitatory ODE which essentially places a nullcline in the trajectory of the excitation/recovery cycle to prevent the excitatory variable from undershooting the resting potential (Rogers, 1992).

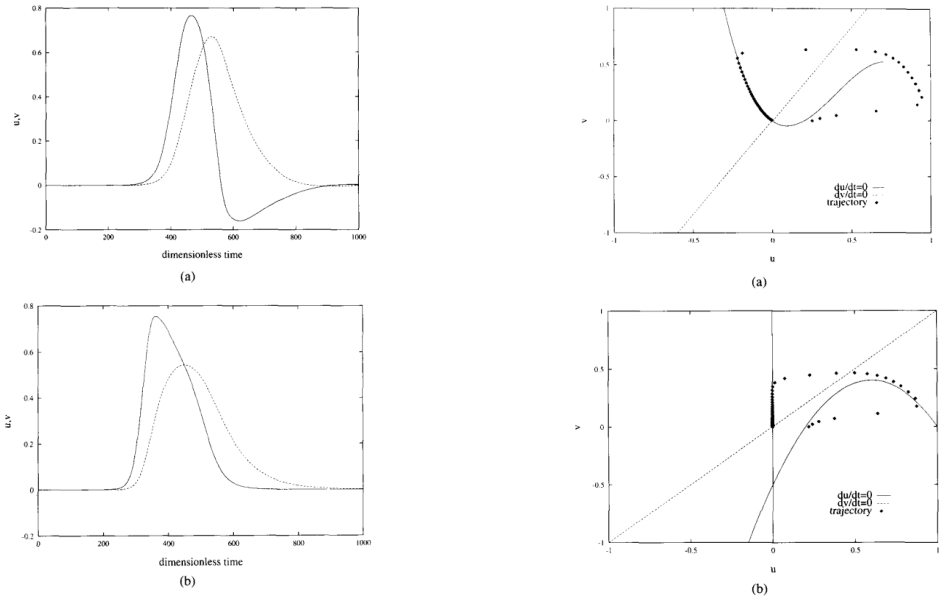

Figure 15: The solid lines of the plots in the left column represent the excitatory variable u; dashed lines represent the recovery variable v. a). The original FitzHugh Nagumo model describing neuronal action potentials exhibits undershoot of the resting potential due to the left branch of the nullcline in the u-v space. b). The MFHN model does not undershoot the resting potential due to the added nullcline at u = 0.

The simulations with FitzHugh Nagumo showed an increase of APD20 and APD90 with increasing strain and a decrease of the APD's and resting potential with increased reversal potential. This conflicts with the Healy-McCulloch model which predicts a decrease in APD 20 and APD90 with increased channel conductance; their increase in channel conductance is taken to be equivalent to increased strain. They also predicted an increase in APD's with increased reversal potential. This difference could be largely due to the simplicity of the FitzHugh Nagumo model. Since there are really only two transmembrane currents involved, the model most likely lacks the fundamental currents that would more realistically produce the behavior seen in the Healy-McCulloch model. The finite simulations clearly show how

strain can largely affect the spatial propagation of the action potential, qualitatively illustrating how arrhythmias due to SACs may occur.

The eight-variable Luo-Rudy model developed in 1991, modified to include a strain-dependent stretch-activated channel, more accurately captured the physiological stretch-response in action potential duration than did the simplified FitzHugh-Nagumo model.

References

Fenton, F., Karma A. (1998) Vortex dynamics in three-dimensional continuous myocardium with fiber rotation: Filament instability and fibrillation. Chaos 8:20-47.

FitzHugh, R. (1961) Impulses and Physiological States in Theoretical Models of Nerve Membrane. Biophysical Journal 1.

Healy, S.N., McCulloch, A.D. (2005) An ionic model of stretch-activated and stretch-modulated currents in rabbit ventricular myocytes. Europace 7:S128-S124.

Lunze, K., Stalhand, J., Leonhardt, S. (2009) Modeling of stretch-activated sarcolemmal channels in smooth muscle cells. International Federation for Medical and Biological Engineering Proceedings 25:740-743.

Luo, C.H., Rudy, Y. (1991) A model of the ventricular cardiac action potential. Depolarization, repolarization, and their interaction. Circulation Research 68:1501-1526.

Puglisi, J.L., Bers, D.M. (2001) LabHEART: an interactive computer model of rabbit ventricular myocyte ion channels and Ca transport. American Journal of Physiology - Cell Physiology 281:2049-2060.